Cellular Instabilities, Sub-Limit Structures, and Edge-Flames in Premixed Counterflows

By John D. Buckmaster[1], & Mark Short[2].

[1] *Department of Aeronautical and Astronautical Engineering, University of Illinois, Urbana, IL 61801*

[2] *Theoretical and Applied Mechanics, University of Illinois, Urbana, IL 61801*

We examine twin premixed flames in a plane counterflow and uncover, in the parameter space, a hitherto unknown domain of cellular instability. This leads us to hypothesize that for small Lewis numbers a 2D steady solution branch bifurcates from the 1D solution branch at a neutral stability point located near the strain-induced quenching point. Solutions on this 2D branch are constructed indirectly by solving an initial value problem in the edge-flame context defined by the multiple-valued bistable 1D solution. Three kinds of solution are found: a periodic array of flame-strings; a single isolated flame-string; and a pair of interacting flame-strings. These structures can exist for values of strain greater than the 1D quenching value, corresponding to sublimit solutions.

1. Introduction

We are concerned in this paper with twin premixed flames in a symmetric counterflow for small values of the Lewis number Le. Specifically we consider $\mathrm{Le} = 0.3$, appropriate for lean hydrogen/air mixtures. We discuss the linear stability of the stationary solution and examine, by numerical means, the nonlinear consequences of a previously unrecognized domain of cellular instability that arises for nearly quenched flames. The nonlinear structures are generated in the context of edge-flame solutions and are robust in the sense that they can survive rates of strain greater than the quenching value for the 1D solution.

Our discussion proceeds as follows. We first briefly summarize the prevailing view on cellular instabilities in strained flames and then identify, by numerical means, a domain of instability in a neighborhood of the quenching point, where the twin flames begin to interact with each other, and the fuel concentration at the symmetry plane is non-zero. We hypothesize that a steady 2D solution branch bifurcates from the neutral stability point on the 1D response curve. Solutions on this 2D branch are sought via numerical solution of an initial-value problem that is capable of generating an edge-flame. For some values of the Damköhler number D (the inverse of the rate of strain), the edge-flame takes the form of an ignition front which trails a stationary periodic structure, an array of flame-strings, and typical solutions of this kind are described. For sufficiently small values of D however, and appropriate initial conditions, a single flame-string or a pair of flame-strings can be generated, hot-spots in the plane of the edge-flame structure. These solutions are discussed in analogy with existing flame-ball

results, and certain mathematical conditions necessary for the existence of an unbounded flame-string are established.

2. The cellular instability of strained flames

It is well known that a small Lewis number deflagration is subject to a Turing instability that leads to unsteady chaotic cellular structure. The instability has been extensively studied in a number of different contexts and configurations, and here we are concerned with twin deflagrations in a symmetric fresh/fresh counterflow.

The simplest way to gain insight into the effect of the flow on the instability is via modifications of the Kuramoto-Sivashinsky (KS) equation. The KS equation has its roots in the dispersion relation derived from the thermal-diffusion model of a deflagration, viz.

$$2K^2(1-K)+\bar{l}\left\{(1-K)^2-4k^2\right\}=0, \quad K=\sqrt{1+4(\lambda+k^2)}, \quad |\arg|<\pi, \tag{2.1}$$

corresponding to perturbations $\sim e^{\lambda t+\mathrm{i}kz}$, where t is time and z is distance measured in the plane of the undisturbed flame. $\bar{l}$ is proportional to $(\mathrm{Le}-1)$ where Le is the Lewis number. As Le is decreased from the value 1, the stability boundary is first reached at $\bar{l}=-1$, $k=0$, and in the neighborhood of this point (2.1) can be approximated by

$$\lambda=-(1+\bar{l})k^2-4k^4. \tag{2.2}$$

From this we see that in the $(\bar{l},k)$ plane λ vanishes on the parabola $(1+\bar{l})+4k^2=0$ and on the line $k=0$, and is a real positive number between these curves.

If the perturbation displacement of the flame-sheet is $F(z,t)$, (2.2) is equivalent to

$$\frac{\partial F}{\partial t}=(1+\bar{l})\frac{\partial^2 F}{\partial z^2}-4\frac{\partial^4 F}{\partial z^4}, \tag{2.3}$$

both a linear evolution equation and a formula for the perturbation to the flame-speed. The first term on the *rhs* arises because of the stretch generated by the corrugations and is Markstein's correction to the flame-speed, destabilizing if $\bar{l}<-1$. The second term is a short-wavelength stabilizing term. Both of them are generated by the physics of the combustion process (diffusion, reaction) whereas the *lhs* is a mere kinematic term. When this kinematic term is modified to account for weak nonlinearities the KS equation is generated, viz.

$$\frac{\partial F}{\partial t}+\frac{1}{2}\left(\frac{\partial F}{\partial z}\right)^2-(1+\bar{l})\frac{\partial^2 F}{\partial z^2}+4\frac{\partial^4 F}{\partial z^4}=0. \tag{2.4}$$

It can of course be derived in a rational fashion via a bifurcation analysis, [1].

The KS equation represents a balance between small terms, and additional physical ingredients can be incorporated provided they are also small. Of particular interest to us is a weak straining flow in the (x,y) plane with flame corrugations only in the z-direction. Now the flame experiences stretch via the flow field, as well as via the corrugations. Also, the spatially varying flow affects the kinematics. A proper accounting for this leads to the modified KS equation [2],

first derived in the axisymmetric context in [3],

$$\frac{\partial F}{\partial t}+\frac{1}{2}\left(\frac{\partial F}{\partial z}\right)^2-(1+\bar{l})\frac{\partial^2 F}{\partial z^2}+4\frac{\partial^4 F}{\partial z^4}+\frac{\alpha}{(1+\bar{l})^2}F=0. \tag{2.5}$$

Here α is the rate of strain. Now the stability boundary is

$$k^2=-\frac{(1+\bar{l})}{8}\pm\frac{1}{8}\sqrt{(1+\bar{l})^2-16\frac{\alpha}{(1+\bar{l})^2}}, \tag{2.6}$$

with stability if $\alpha/(1+\bar{l})^4 > 1/16$. In other words, for any fixed value of $\bar{l}$, stability can be achieved by imposing a sufficiently large strain. Otherwise, in the neighbourhood of the turning point determined by (2.6), weak instability leads to finite stationary corrugations of wavenumber

$$k_c=\sqrt{-\frac{(1+\bar{l})}{8}}, \tag{2.7}$$

as can easily be shown by a bifurcation analysis of (2.5), e.g. [2].

In summary, an unstrained small Lewis number flame exhibits unsteady cellular structure; this structure becomes fixed and periodic for large enough strain; and can be entirely suppressed for even larger strain. However, it turns out that this is not the full story, for we have discovered that the instability can return for large values of the straining rate.

3. Cellular instability near the quenching point

An appropriate model for the one-dimensional flame in a counterflow is described by the boundary-value problem

$$\underline{0<x<\infty}\quad -x\frac{\mathrm{d}T}{\mathrm{d}x}=\frac{\mathrm{d}^2T}{\mathrm{d}x^2}+DYe^{-\theta/T},\quad -x\frac{\mathrm{d}Y}{\mathrm{d}x}=\frac{1}{\mathrm{Le}}\frac{\mathrm{d}^2Y}{\mathrm{d}x^2}-DYe^{-\theta/T};$$
$$\frac{\mathrm{d}T}{\mathrm{d}x}=0,\ \frac{\mathrm{d}Y}{\mathrm{d}x}=0 \text{ at } x=0;\quad T\to T_f,\ Y\to 1 \text{ as } x\to\infty. \tag{3.1}$$

Here D, the Damköhler number, is proportional to α^{-1} where α is the rate of strain, and the scalings are such that the nondimensional adiabatic flame temperature is $(1+T_f)$. These equations can be solved using a shooting method, and in Fig. 1 we show variations of the center-line ($x=0$) temperature T_m with Damköhler number. Within a framework that resolves the cold-boundary difficulty (a cut-off temperature, for example) there is an additional solution, the quenched solution $T_m=T_f$. Because θ/T_f is large, the resolution need not be made explicit.

We see then that for D greater than the quenching value D_e ($D_e=3.938\times10^5$, with a corresponding value of T_m equal to 1.761) there are three solutions, of which the middle one is assuredly unstable, and for values of D smaller than D_e there is a single stable solution. Quenching occurs because of interaction between the reaction-zone and the symmetry plane $x=0$. In the asymptotic context $\theta\to\infty$ it comes about because of interaction with the exponentially decaying solution on the burnt side of the flame-sheet, a delicate matter that has only recently been described, [4].

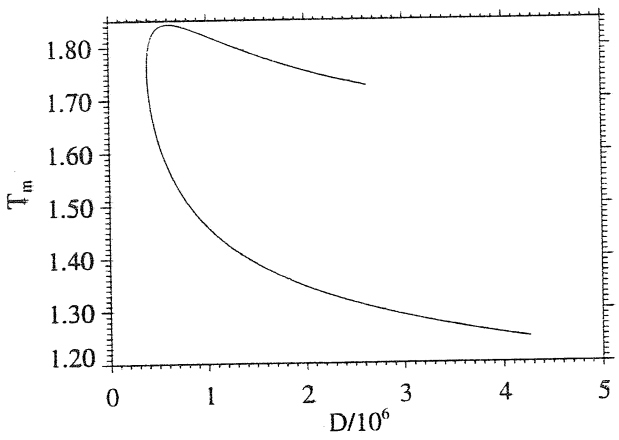

Figure 1. Variations of the maximum temperature with D for the 1D flame; $Le = 0.3$, $\theta = 16$, $T_f = 0.2$.

The stability of the solutions can be examined numerically via a normal-mode analysis. To this end we write

$$T = T^*(x) + \epsilon T'(x)\mathrm{e}^{\mathrm{i}kz+\lambda t}, \quad Y = Y^*(x) + \epsilon Y'(x)\mathrm{e}^{\mathrm{i}kz+\lambda t}, \quad \epsilon\theta \ll 1, \tag{3.2}$$

where T^* and Y^* are the steady solutions. Adding time derivatives to (3.1), replacing $\mathrm{d}^2/\mathrm{d}x^2$ by $\mathrm{d}^2/\mathrm{d}x^2 + \mathrm{d}^2/\mathrm{d}z^2$, and linearizing then leads to the system

$$\begin{aligned} &\frac{\mathrm{d}^2T'}{\mathrm{d}x^2} + x\frac{\mathrm{d}T'}{\mathrm{d}x} - (k^2+\lambda)T' + DY'\mathrm{e}^{-\theta/T^*} + D\frac{Y^*}{T^{*2}}\theta T'\mathrm{e}^{-\theta/T^*} = 0, \\ &\frac{1}{\mathrm{Le}}\frac{\mathrm{d}^2Y'}{\mathrm{d}x^2} + x\frac{\mathrm{d}Y'}{\mathrm{d}x} - (\frac{k^2}{\mathrm{Le}}+\lambda)Y' - DY'\mathrm{e}^{-\theta/T^*} - D\frac{Y^*}{T^{*2}}\theta T'\mathrm{e}^{-\theta/T^*} = 0, \end{aligned} \tag{3.3}$$

with boundary conditions,

$$\frac{\mathrm{d}T'}{\mathrm{d}x} = 0, \quad \frac{\mathrm{d}Y'}{\mathrm{d}x} = 0 \text{ at } x = 0; \quad T' \to 0, \ Y' \to 0 \text{ as } x \to \infty. \tag{3.4}$$

(We restrict attention to perturbations that are even in x). Upon discretization, a generalized matrix eigenvalue problem is obtained of the form

$$\mathbf{A}y = \lambda \mathbf{B}y \tag{3.5}$$

which can be solved using standard packages. In this way we find that for each value of D between D_e and a value $D_0(= 4.30 \times 10^5)$ solutions on the upper branch of Fig. 1 define real positive eigenvalues in a finite wavenumber interval $(k_1(D), k_2(D))$ where $k_1 > 0$, Figs. 2, 3.

We believe that a 2-D solution branch bifurcates from the neutral stability point of Fig. 2, although we have not calculated it. Where such a branch wanders remains to be seen, but we argue that there is nothing that forces it to stay to the right of D_e. Indeed, because we expect the solutions on this branch to correspond to highly curved cellular flames, they will be more robust than the plane flame, better able to resist the straining flow, because of Lewis-number curvature effects. We shall construct solutions on the branch by solving a two-dimensional initial-value problem, one that defines an edge-flame.

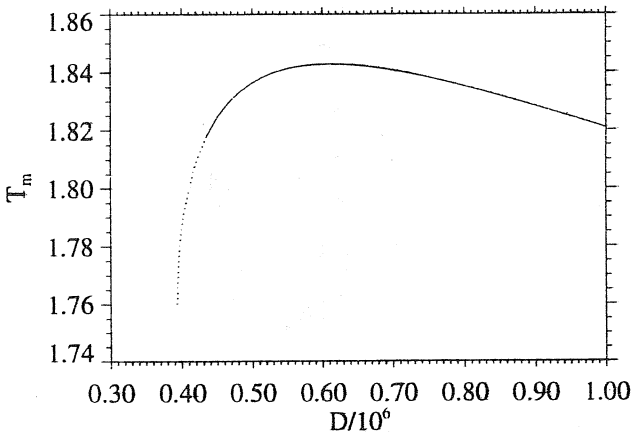

Figure 2. The near-quenching region of cellular instability in the T_m - D response diagram; Le $= 0.3$, $\theta = 16$, $T_f = 0.2$.

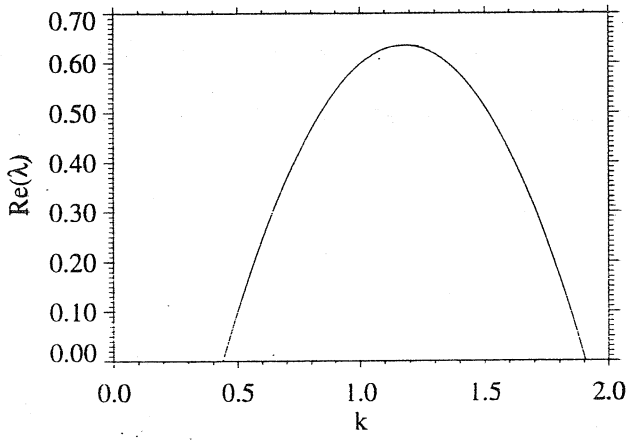

Figure 3. Variations with k of the eigenvalue with the biggest real part, $D = 4.031 \times 10^5$.

4. Edge-flames

Edge-flames can be thought of as two-dimensional structures that effect a transition between two one-dimensional solutions, one corresponding to weak burning, the other to strong burning. In the present context the strong solution can be defined by the upper branch of Fig. 1 (so that $D > D_e$) and the weak solution by the quenched solution $T_m = T_f$. This definition is unnecessarily restrictive - as we shall see the strong solution can itself be two-dimensional, and for an anchored edge-flame the weak solution may not be fully realized between the edge-flame structure and the anchor - but it provides a nominal framework for an essential understanding of these creatures. A significant amount of work has been done on edge-flames in non-premixed combustion, e.g. [5], [6], including the analysis of one-dimensional models that elucidate their behaviour [7], and edge-flames

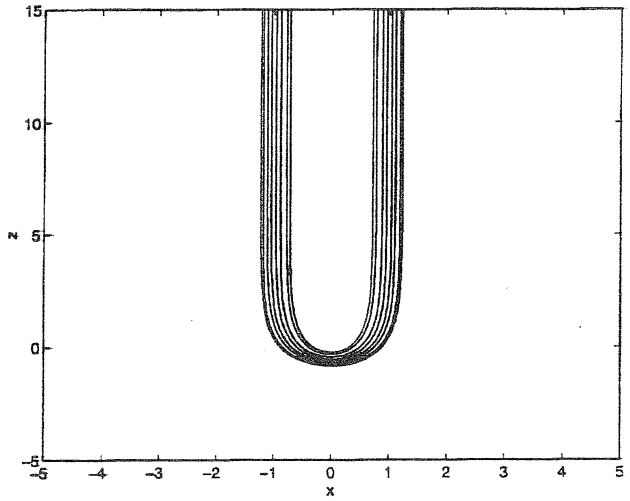

Figure 4. Reaction-rate contours for an ignition front, Le = 1, from [4]. The front travels downwards, igniting the mixture ahead of it. A failure wave corresponds to upward movement, quenching by the cold mixture.

in premixed combustion have recently been described for the first time, [4], [8], albeit for a Lewis number of 1.

The edge-flame model corresponding to (3.1) is described by the equations

$$\begin{aligned}
&\frac{\partial T}{\partial t} = x\frac{\partial T}{\partial x} + \frac{\partial^2 T}{\partial x^2} + \frac{\partial^2 T}{\partial z^2} + DYe^{-\theta/T},\\
&\frac{\partial Y}{\partial t} = x\frac{\partial Y}{\partial x} + \frac{1}{\mathrm{Le}}\left(\frac{\partial^2 Y}{\partial x^2} + \frac{\partial^2 Y}{\partial z^2}\right) - DYe^{-\theta/T};\\
&\frac{\partial T}{\partial x} = 0 = \frac{\partial Y}{\partial x} \text{ at } x = 0; \qquad T \to T_f,\ Y \to 1 \text{ as } x \to \infty;\\
&T \to T^*(x),\ Y \to Y^*(x) \text{ as } z \to \infty, \qquad T \to T_f,\ Y \to 1 \text{ as } z \to -\infty.
\end{aligned} \tag{4.1}$$

Here T^*, Y^* is the steady solution on the upper branch for the assigned value of D. A smooth interpolation between $\{T^*,\ Y^*\}$ and the quenched solution is used to define initial conditions. And the boundary conditions at $z = \pm\infty$ which are imposed at finite values of z at $t = 0$ are switched to Neumann conditions ($\partial T/\partial z = \partial Y/\partial z = 0$) when $t > 0$. As in the stability analysis, we restrict attention to solutions that are even in x.

The flame described by these equations has a thick edge, a bridging of the two reaction zones defined by the underlying one-dimensional problem, and either propagates as an ignition front or as a failure wave. (Thin-edge-flames, associated with a single reaction zone, are also described in [4], [8]). Reaction rate contours of a typical ignition front (traveling downwards), duplicated from [4], are shown in Fig.4

It is a common characteristic of edge-flames that both positive and negative edge speeds occur, according to the value of D. Large values of D generate positive speeds (ignition fronts) whereas values of D near the quenching value generate

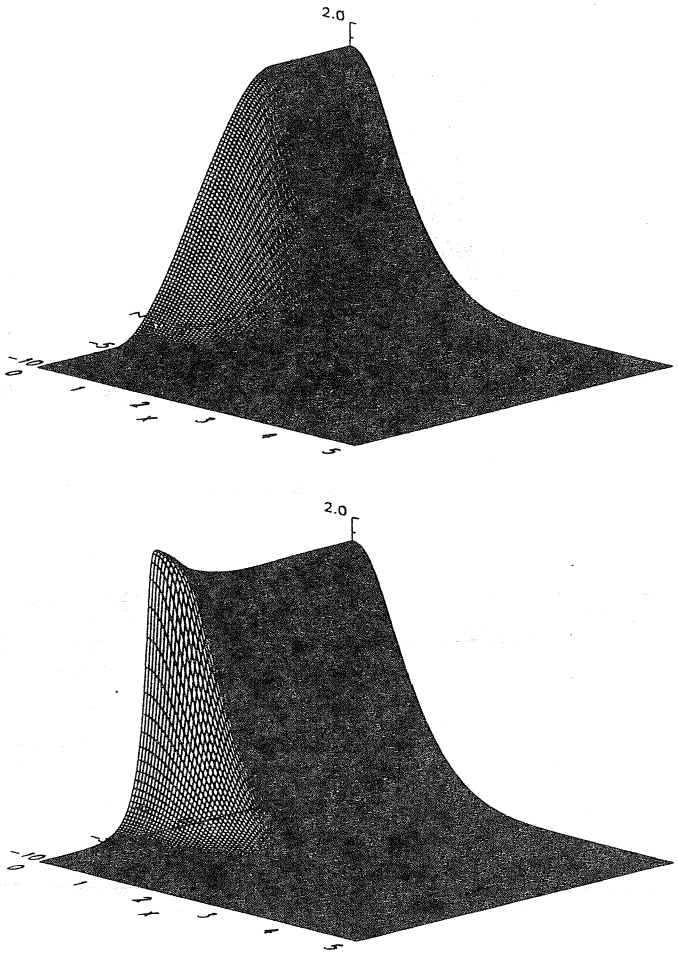

Figure 5. (a,b). Temperature topography at $t = 0,\ 10$; $D = 5.611 \times 10^5$, Le $= 0.3$, $\theta = 16$, $T_f = 0.2$.

negative speeds (failure waves). However it was recently shown that, for exceptional circumstances, positive speeds can be obtained even down to the quenching value [4]. It is not surprising that the present problem is one of these exceptions, for at small values of Le the curvature of the edge (cf. Fig. 4) will enhance the local reaction. So strong is this effect, in fact, that ignition fronts can exist even for values of D less than the quenching value of D_e. Such a front can not trail a one-dimensional structure (cf. Fig. 4) as this can not survive the large strain. Rather, it trails a two-dimensional structure corresponding to a point on the 2D bifurcating branch of Fig. 2.

5. Numerical results

The problem defined by (4.1) has been solved using 4th-order spatial discretization, and third-order Runge-Kutta time integration. Figs 5a,b show the temperature topography at $t = 0,\ 10$ for $D = 5.611 \times 10^5$, a value greater than D_0, the

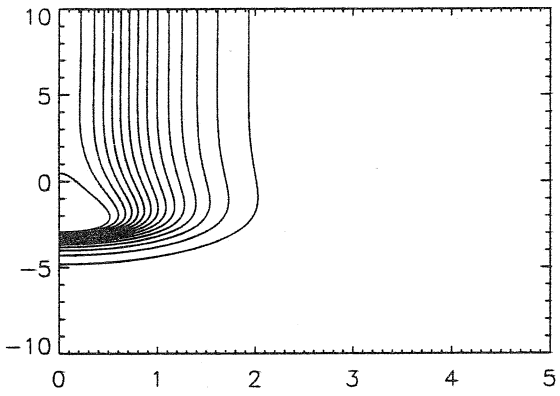

Figure 5. (c). Temperature contours at $t = 10$.

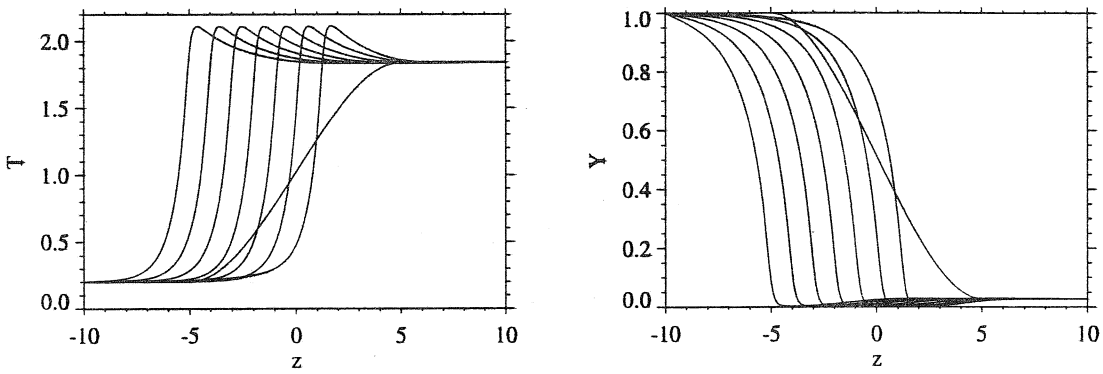

Figure 5. (d,e). T and Y profiles at the symmetry plane $x = 0$, $t = 0(2), 14$.

value at the neutral stability point of Fig. 2. Fig. 5a shows the initial temperature distribution. The solution along the edge $z = 10$ is the strong-burning 1-D solution; along the edge $z = -10$ the solution is the quenched one. By a time $t = 10$ a fully-developed ignition front has emerged (Fig. 5b) which clearly shows an enhanced temperature at the edge arising from the Lewis-number - curvature effect (see also the temperature contours in Fig. 5c). The front is traveling at a well defined speed, as is clear from Figs 5d, 5e which show variations of T and Y along the symmetry plane $x = 0$. Note from Fig. 5e that there is residual unburnt fuel behind the trailing 1D flame ($x = 0, z = +10$). This reflects the fact that D is small enough for there to be interaction between the reaction zone and the symmetry plane.

We turn now to results for $D = 4.031 \times 10^5$, a value lying between D_e and D_0. Then the underlying 1D structure exists but is unstable. Fig. 6a shows a well developed ignition front at a time $t = 60$ (the temperature contours are shown in Fig. 6b) and the T and Y profiles at $x = 0$ are shown in Figs. 6c,d for $t = 0(4), 60$. Strong stationary cellular structures are seen, a train of flame-string

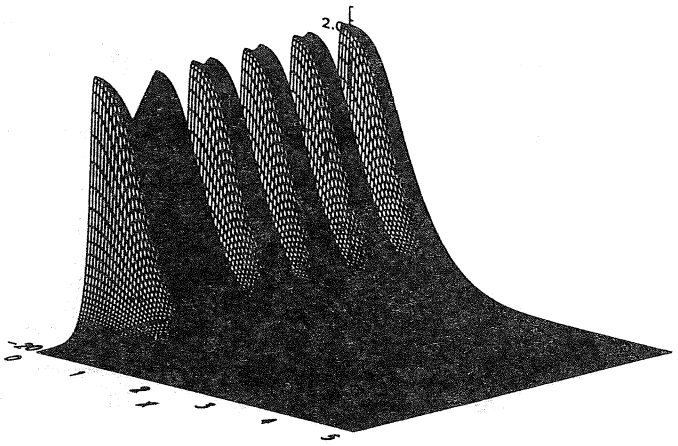

Figure 6. (a). Temperature topography at $t = 60$; $D = 4.031 \times 10^5$, Le $= 0.3$, $\theta = 16$, $T_f = 0.2$.

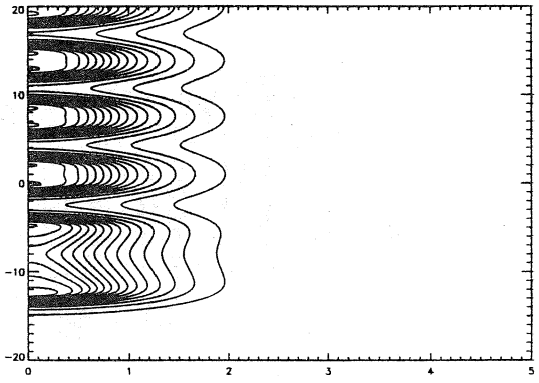

Figure 6. (b) Temperature contours at $t = 60$.

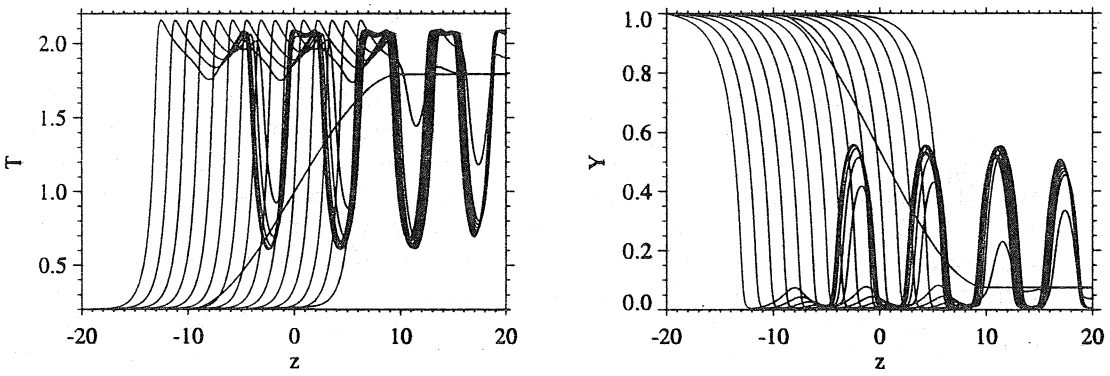

Figure 6. (c,d). T and Y profiles at the symmetry plane $x = 0$, $t = 0(4)60$.

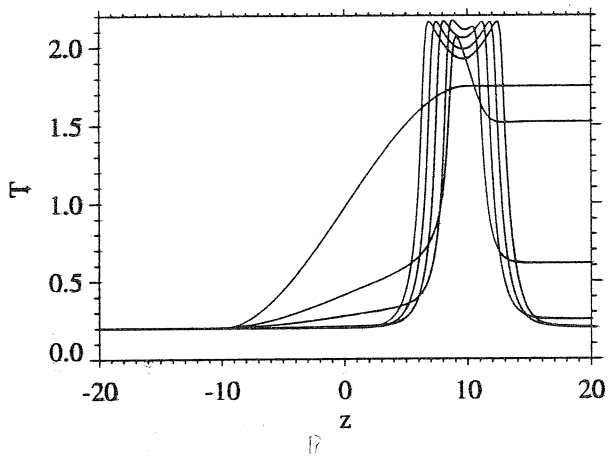

Figure 7. (a). T profiles at the symmetry plane $x = 0$, $t = 0,\ 1,\ 2(2)\ 8$; $D = 3.794 \times 10^5$, Le $= 0.3$, $\theta = 16$, $T_f = 0.2$.

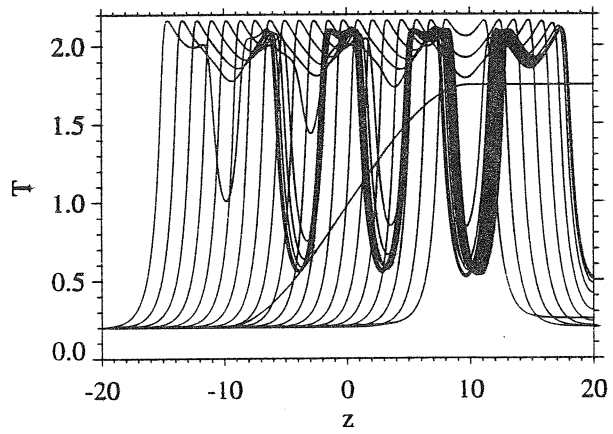

Figure 7. (b). T profiles at the symmetry plane $x = 0$, $t = 0(4),\ 80$.

like structures (we shall say something about flame-strings in a later section). These are continuously generated as the front advances, by the splitting of the leading high temperature cell. Thus at $t = 60$ we see in Fig. 6c a cell, an interval bounded by a temperature maximum at $z \approx -12.5$ and $z \approx -5$, splitting at $z \approx -8$. We believe that in an unbounded domain, and in the limit $t \to \infty$, the train would be periodic with an intrinsically defined wavelength. Thus the difference in the nature of the rightmost crest from the other ones in Fig. 6d is due to interaction with the computational boundary at $z = 20$, where Neumann conditions are applied. We arrived at this conclusion by examining different sized domains. Similar results to those described in this paragraph are obtained when $D = 3.951 \times 10^5$.

The value $D = 3.794 \times 10^5$ is smaller than D_e, and results for this case were obtained by using the $t = 0$ prescription (smooth) at $D = 3.951 \times 10^5$ for the initial

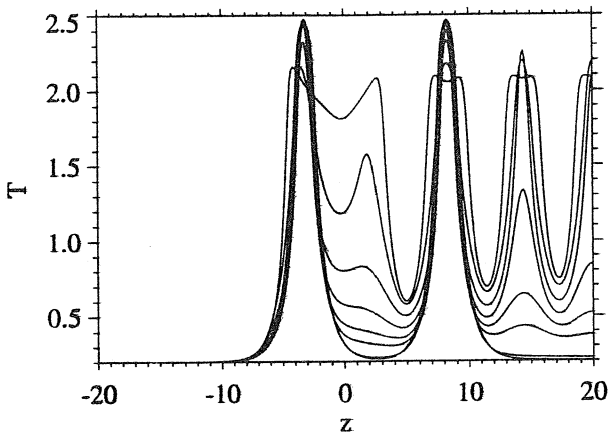

Figure 8. T profiles at the symmetry plane $x = 0$, $t = 0(1)$, 5; $t = 9, 13$ (merged); Le $= 0.3$, $\theta = 16$, $T_f = 0.2$, $D = 1.343 \times 10^5$.

conditions. Figure 7a shows temperature profiles at $x = 0$ for $t = 0,\ 1,\ 2(2), 8$ and reveals a rapid decay of the post-edge one-dimensional structure forced by the small value of D. However the edge not only survives but its vigor increases. It then acts as an ignition source for two ignition fronts, one propagating to the right, the other to the left, and between which is left a train of stationary flame-strings, Fig. 7b. Sublimit solutions of this kind can be generated for a range of values of D smaller than D_e.

In addition to the sublimit solutions characterized by a train of cellular structures (flame strings) there are also solutions in which the edge survives but fails to act as an ignition source. This occurs for a range of values of D smaller than those that generate the train. An example is shown in Fig. 8, in which initial conditions are defined by the solution for $D = 3.951 \times 10^5$ at $t = 40$ (Fig. 7b) but D has the value 1.343×10^5. The post-edge structure collapses, leaving two interacting stationary flame-strings.

Single flame-strings can also be generated. The solution in Fig. 9 is found by starting with one of the solution curves ($t = 4$) from Fig 7a, but with $D = 1.976 \times 10^5$. It seems that there are a number of solution branches when $D < D_e$, and we have not attempted to find all of them; which one is attained depends both on the value of D, and on the initial conditions. Not surprisingly, the single string (nor any other number) can not survive arbitrarily large values of strain, and at small Damköhler numbers complete quenching occurs (Fig. 10).

6. Some remarks on flame-strings

A discussion of flame-strings is best started with a discussion of flame-balls, to which they are closely related, and which are well understood. Flame-balls are stationary spherical flames that are observed in small Lewis number mixtures, [9]. Their stability requires a heat-loss mechanism either through radiation, heat conduction (to a cold-boundary, for example), or convection. Radiation losses are undoubtedly the key mechanism in the observed balls, but here we are concerned with convective losses generated by placing the ball in a weak planar straining

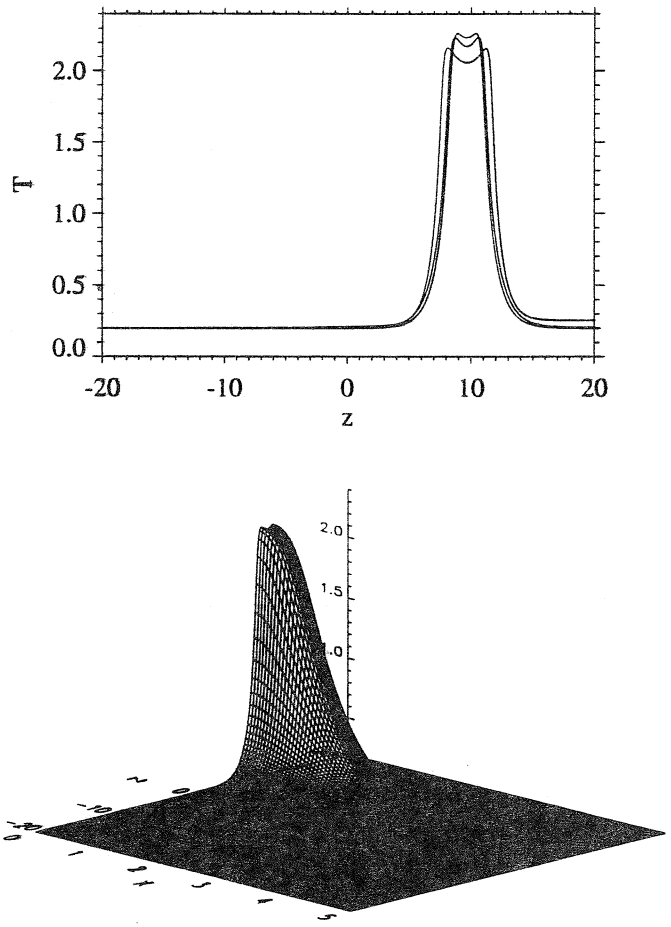

Figure 9. (a) T profiles at the symmetry plane $x = 0$, $t = 0, 2$; $t = 10, 20$ (merged). (b) Temperature topography at $t = 20$; Le $= 0.3$, $\theta = 16$, $T_f = 0.2$, $D = 1.976 \times 10^5$.

flow. The flow is both a friend and an enemy: For certain values of the strain rate it is stabilizing, but at high enough rates it quenches the ball.

The cylindrical counterpart to a flame-ball is a flame-string, [10]. (In choosing the name 'flame-string' the alternative 'flame-cylinder' was rejected since observed structures do not necessarily have straight axes; and the metaphorical ball-string connection suggested by the pulling of the string from the ball was impossible to resist). A steady flame-string solution bounded at infinity can not be found in the absence of a flow field because the point source/sink solution of Laplace's equation is $\ln r$ (r=cylindrical radius). Later we shall show that the 'infinity problem at infinity' is eliminated by the presence of the straining flow. And if we assume that strain affects a string in the same fashion that it affects a ball, we conclude that a single stable string can exist for some strain rates, and this string will be quenched for some other (larger) strain rates, [11]. This provides an explanation of our single string results, Figs. 9 and 10.

Generation of a train of strings presumably corresponds to an instability of the

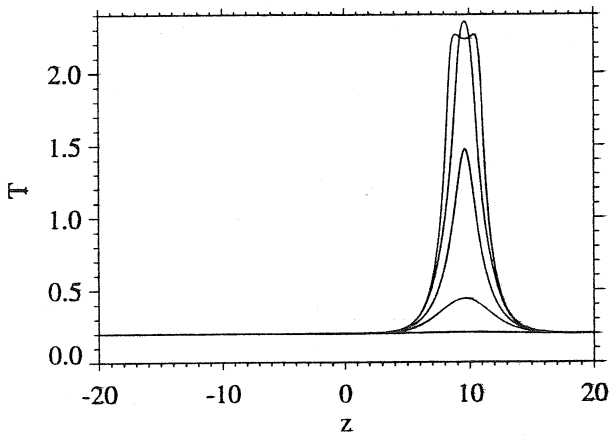

Figure 10. (a). T profiles at the symmetry plane $x = 0$ during single string decay; $t = 0, 0.5, 1, 2, 5$; $t = 0.5$, Le $= 0.3$, $\theta = 16$, $T_f = 0.2$, $D = 7.903 \times 10^4$. Initial conditions correspond to the late-time solution Fig. 9(b)

single string solution. The latter acts as a non-isotropic ignition source, generating a flame-sheet of growing width that is itself unstable, collapsing into regularly spaced strings. There is an analogy with the observed generation of a flame-string from a flame-ball: The ball extends to form the string, but the string is 3-D unstable and collapses to form a train of balls [12].

7. Flame-string mathematics

It is not our intention here to provide an asymptotic description of flame-strings in a straining flow, a counterpart to the flame-ball analysis of [12]. Indeed we are not certain that such an analysis is possible, as there are substantial technical difficulties. Instead, we wish merely to show that a point source in a straining flow generates a field that vanishes at infinity, that indeed the straining flow is sufficient to eliminate the logarithmic embarrassment that arises when there is no velocity field. To this end, consider the problem

$$-x\frac{\partial\phi}{\partial x} = \frac{\partial^2\phi}{\partial x^2} + \frac{\partial^2\phi}{\partial z^2} + \delta(x)\delta(z), \quad \phi \to 0 \text{ as } r = \sqrt{x^2+z^2} \to \infty. \tag{7.1}$$

The large r behavior of ϕ defines the large r behavior of the T and Y fields generated by a single flame-string.

A Fourier transform in z, followed by inversion, yields the solution

$$\phi = \frac{e^{-x^2/2}}{\pi 2\sqrt{2}} \int_0^\infty \mathrm{d}k \cos(kz) f(k,x), \tag{7.2}$$

where

$$f(k,x)\Gamma(1+k^2/2) \equiv \int_0^\infty \mathrm{d}t\, e^{-|x|\sqrt{2t}-t} t^{k^2/2-1/2}. \tag{7.3}$$

f decays monotonically with k, vanishes as $k \to \infty$, and is an even function of k so that all its derivatives vanish at $k = 0$. Thus if we integrate (7.2) by parts

we deduce that ϕ must decay faster than any power of z as $|z| \to \infty$, since terms generated in this way have the form

$$\begin{aligned} &\frac{\partial^{n-1} f(k,x)}{\partial k^{n-1}} \frac{\cos(kz)}{z^n} \Big|_{k=0}^{\infty} && \text{n even;} \\ &\frac{\partial^{n-1} f(k,x)}{\partial k^{n-1}} \frac{\sin(kz)}{z^n} \Big|_{k=0}^{\infty} && \text{n odd.} \end{aligned} \tag{7.4}$$

An explicit demonstration is possible when $x = 0$ for then

$$\phi = \frac{1}{\pi 2\sqrt{2}} \int_0^\infty \mathrm{d}k \, \cos(kz) \frac{\Gamma(1/2 + k^2/2)}{\Gamma(1 + k^2/2)} = \frac{1}{\pi 2\sqrt{2}} \mathrm{Re} \int_0^\infty \mathrm{d}k e^{ikz} \frac{\Gamma(1/2 + k^2/2)}{\Gamma(1 + k^2/2)}. \tag{7.5}$$

By rotating the integration path to the positive imaginary axis and evaluating the residues of the poles generated by $\Gamma(1/2 + k^2/2)$ on that axis, we find

$$\phi = \frac{1}{2\sqrt{2}} \sum_{n=0}^{\infty} (-1)^n \frac{e^{-z\sqrt{1+2n}}}{n! \sqrt{1+2n}\, \Gamma(1/2 - n)} \sim \frac{e^{-z}}{2\sqrt{2\pi}} + O(e^{-\sqrt{3}z}). \tag{7.6}$$

The exponential decay strongly suggests that the problem for an unbounded train of flame-strings is also well posed.

8. Concluding Remarks

We have shown that driving a small Lewis-number deflagration close to extinction in a symmetric straining flow can generate strong cellular structures, flame-strings. These have their roots in a previously unrecognized linear instability that arises as the deflagration weakens by interaction with the symmetry plane. Moreover, the structures are robust in the sense that they can survive straining rates greater than the 1D quenching value, a consequence of their strong curvature. This type of robustness is familiar in flames subject to radiation losses, for it has long been known that hydrogen/air mixtures can support small curved structures for mixture strengths too weak to support plane deflagrations. But it has not previously been clearly addressed in the context of straining flows.

The implications for the calculation of turbulent hydrogen/air flames are daunting, for it is clear that the usual flamelet libraries, constructed in the context of the response of a plane flame to a straining flow, incorporate only part of the physics when Le is small. This is true not only for premixed combustion, but also for non-premixed combustion. In the latter case, local quenching because of scalar dissipation can lead to mixing, and the mixtures can support sublimit structures.

The cellular structures we have described are cylindrical in nature, a consequence of the geometric constraints of our model. If we permitted flame corrugations in the y-direction it is possible that the strings would break up into balls, although not necessarily, since the stretch in the y-direction would tend to suppress the corrugations. But certainly in the non-idealized complexity that characterizes most physical flows we would expect that the physics that we have described here would lead, not to strings, but to balls.

The calculations that we report here are all for $Le = 0.3$, and we have not systematically explored what happens for other values, but we have generated a

few additional results. Thus we know that for $Le = 0.5$, $D = D_e$ (a value different from the current one), the edge-speed is positive, and cells form, as here. Also, for $Le = 0.7$, $D = D_e$, the edge-speed is negative, corresponding to a failure wave, and we observed no cell formation before the edge left the computational domain.

9. Acknowledgments

This work was supported by AFOSR and by the NASA-Lewis Research Center.

References

[1] Sivashinsky, G.I. 1983 *Ann. Rev. Fluid Mech.* **15** 179–99.

[2] Buckmaster, J.D. & Ludford, G.S.S. 1983 Lectures on Mathematical Combustion. SIAM, Philadelphia.

[3] Sivashinsky, G.I., Law, C.K., & Joulin, G. 1982 *Combust. Sci. Techn.* **28** 155–160.

[4] Vedarajan, T.G., Buckmaster, J.D. & Ronney, P.D. 1998 27th International Symposium on Combustion, to appear.

[5] Dold, J.W., Hartley, L.J., & Green, D. 1991 In 'Dynamical Issues in Combustion Theory,' IMA Volumes in Mathematics and its Applications, eds. Paul C. Fife, A. Liñàn, & F. Williams, Springer, New York, 83–105.

[6] Kioni, P.N., Rogg, B., Bray, K.N.C., & Liñàn, A. 1993 *Combust. Flame* **95** 276–290.

[7] Buckmaster, J.D. 1997 *J. Eng. Math.* **31** 269–284.

[8] Vedarajan, T.G & Buckmaster, J.D. 1998 *Combust. Flame* **114** 267–273.

[9] Ronney, P.D. 1990 *Combust. Flame* **82** 1–14.

[10] Buckmaster, J.D., 1992 *Combust. Sci. Tech.* **84** 167–176.

[11] Buckmaster, J.D. & Joulin, J. 1991 *J. Fluid Mech.* **227** 407–427.

[12] Ronney, P.D., Whaling, K.N., Abbud-Madrid, A., Gatto, J.L., & Pisowicz, V.L. 1994 *AIAA J.* **32** 569–577.

List of Recent TAM Reports

No.	Authors	Title	Date
805	Jonnalagadda, K., G. E. Kline, and N. R. Sottos	Local displacements and load transfer in shape memory alloy composites—*Experimental Mechanics* **37**, 82–90 (1997)	Aug. 1995
806	Nimmagadda, P. B. R., and P. Sofronis	On the calculation of the matrix–reinforcement interface diffusion coefficient in composite materials at high temperatures—*Acta Metallurgica et Materialia* **44**, 2711–2716 (1996)	Aug. 1995
807	Carlson, D. E., and D. A. Tortorelli	On hyperelasticity with internal constraints—*Journal of Elasticity* **42**, 91–98 (1966)	Aug. 1995
808	Sayre, T. L., and D. N. Riahi	Oscillatory instabilities of the liquid and mushy layers during solidification of alloys under rotational constraint—*Acta Mechanica* **121**, 143–152 (1997)	Sept. 1995
809	Xin, Y.-B., and K. J. Hsia	Simulation of the brittle–ductile transition in silicon single crystals using dislocation mechanics—*Acta Metallurgica et Materialia* **45**, 1747–1759 (1997)	Oct. 1995
810	Ulysse, P., and R. E. Johnson	A plane-strain upper-bound analysis of unsymmetrical single-hole and multi-hole extrusion processes	Oct. 1995
811	Fried, E.	Continua described by a microstructural field—*Zeitschrift für angewandte Mathematik und Physik* **47**, 168–175 (1996)	Nov. 1995
812	Mittal, R., and S. Balachandar	Autogeneration of three-dimensional vortical structures in the near wake of a circular cylinder	Nov. 1995
813	Segev, R., E. Fried, and G. de Botton	Force theory for multiphase bodies—*Journal of Geometry and Physics* **20**, 371–392 (1996)	Dec. 1995
814	Weaver, R. L.	The effect of an undamped finite-degree-of-freedom "fuzzy" substructure: Numerical solutions and theoretical discussion—*Journal of the Acoustical Society of America* **100**, 3159–3164 (1996)	Jan. 1996
815	Haber, R. B., C. S. Jog, and M. P. Bendsøe	A new approach to variable-topology shape design using a constraint on perimeter—*Structural Optimization* **11**, 1–12 (1996)	Feb. 1996
816	Xu, Z.-Q., and K. J. Hsia	A numerical solution of a surface crack under cyclic hydraulic pressure loading—*ASME Journal of Tribology* **119**, 637–645 (1997)	Mar. 1996
817	Adrian, R. J.	Bibliography of particle velocimetry using imaging methods: 1917–1995—*Produced and distributed in cooperation with TSI, Inc., St. Paul, Minn.*	Mar. 1996
818	Fried, E., and G. Grach	An order-parameter based theory as a regularization of a sharp-interface theory for solid–solid phase transitions—*Archive for Rational Mechanics and Analysis* **138**, 355–404 (1997)	Mar. 1996
819	Vonderwell, M. P., and D. N. Riahi	Resonant instability mode triads in the compressible boundary-layer flow over a swept wing—*International Journal of Engineering Science* **36**, 599–624 (1998)	Mar. 1996
820	Short, M., and D. S. Stewart	Low-frequency two-dimensional linear instability of plane detonation—*Journal of Fluid Mechanics* **340**, 249–295 (1997)	Mar. 1996
821	Casagranda, A., and P. Sofronis	On the scaling laws for the consolidation of nanocrystalline powder compacts—Proceedings of the *IUTAM Symposium on the Mechanics of Granular and Porous Materials*, N. A. Fleck and A. C. F. Cocks, eds. The Netherlands: Kluwer Academic Publishers, 105–116 (1997)	Apr. 1996
822	Xu, S., and D. S. Stewart	Deflagration-to-detonation transition in porous energetic materials: A comparative model study—*Journal of Engineering Mathematics* **31**, 143–172 (1997)	Apr. 1996
823	Weaver, R. L.	Mean and mean-square responses of a prototypical master/fuzzy structure—*Journal of the Acoustical Society of America* **101**, 1441–1449 (1997)	Apr. 1996
824	Fried, E.	Correspondence between a phase-field theory and a sharp-interface theory for crystal growth—*Continuum Mechanics and Thermodynamics* **9**, 33–60 (1997)	Apr. 1996
825	Students in TAM 293–294	Thirty-third student symposium on engineering mechanics, J. W. Phillips, coordinator: Selected senior projects by W. J. Fortino II, A. A. Mordock, and M. R. Sawicki	May 1995

List of Recent TAM Reports (cont'd)

No.	Authors	Title	Date
826	Riahi, D. N.	Effects of roughness on nonlinear stationary vortices in rotating disk flows—*Mathematical and Computer Modeling* **25**, 71–82 (1997)	June 1996
827	Riahi, D. N.	Nonlinear instabilities of shear flows over rough walls, *Far East Journal of Applied Mathematics*, in press (1998)	June 1996
828	Weaver, R. L.	Multiple scattering theory for a plate with sprung masses, mean responses—*Journal of the Acoustical Society of America* **101**, 3466–3414 (1997)	July 1996
829	Moser, R. D., M. M. Rogers, and D. W. Ewing	Self-similarity of time-evolving plane wakes *Journal of Fluid Mechanics*, in press (1998)	July 1996
830	Lufrano, J. M., and P. Sofronis	Enhanced hydrogen concentrations ahead of rounded notches and cracks: Competition between plastic strain and hydrostatic stress—*Acta Metallurgica et Materialia*, in press (1998)	July 1996
831	Riahi, D. N.	Effects of surface corrugation on primary instability modes in wall-bounded shear flows	Aug. 1996
832	Bechel, V. T., and N. R. Sottos	Application of debond length measurements to examine the mechanics of fiber pushout	Aug. 1996
833	Riahi, D. N.	Effect of centrifugal and Coriolis forces on chimney convection during alloy solidification—*Journal of Crystal Growth* **179** , 287–296 (1997)	Sept. 1996
834	Cermelli, P., and E. Fried	The influence of inertia on configurational forces in a deformable solid—*Proceedings of the Royal Society of London A* **453**, 1915–1927 (1997)	Oct. 1996
835	Riahi, D. N.	On the stability of shear flows with combined temporal and spatial imperfections	Oct. 1996
836	Carranza, F. L., B. Fang, and R. B. Haber	An adaptive space–time finite element model for oxidation-driven fracture, *Computer Methods in Applied Mechanics and Engineering*, in press (1997)	Nov. 1996
837	Carranza, F. L., B. Fang, and R. B. Haber	A moving cohesive interface model for fracture in creeping materials, *Computational Mechanics* **19**, 517–521 (1997)	Nov. 1996
838	Balachandar, S., R. Mittal, and F. M. Najjar	Properties of the mean wake recirculation region in two-dimensional bluff body wakes—*Journal of Fluid Mechanics*, in press (1997)	Dec. 1996
839	Ti, B. W., W. D. O'Brien, Jr., and J. G. Harris	Measurements of coupled Rayleigh wave propagation in an elastic plate—*Journal of the Acoustical Society of America* **102**, 1528–1531	Dec. 1996
840	Phillips, W. R. C.	On finite-amplitude rotational waves in viscous shear flows—*Studies in Applied Mathematics* **100**, in press (1998)	Jan. 1997
841	Riahi, D. N.	Direct resonance analysis and modeling for a turbulent boundary layer over a corrugated surface—*Acta Mechanica*, in press (1998)	Jan. 1997
842	Liu, Z.-C., R. J. Adrian, C. D. Meinhart, and W. Lai	Structure of a turbulent boundary layer using a stereoscopic, large format video-PIV—*Developments in Laser Techniques and Fluid Mechanics*, 259–273 (1997)	Jan. 1997
843	Fang, B., F. L. Carranza, and R. B. Haber	An adaptive discontinuous Galerkin method for viscoplastic analysis—*Computer Methods in Applied Mechanics and Engineering* **150**, 191–198 (1997)	Jan. 1997
844	Xu, S., T. D. Aslam, and D. S. Stewart	High-resolution numerical simulation of ideal and non-ideal compressible reacting flows with embedded internal boundaries—*Combustion Theory and Modeling* **1**, 113–142 (1997)	Jan. 1997
845	Zhou, J., C. D. Meinhart, S. Balachandar, and R. J. Adrian	Formation of coherent hairpin packets in wall turbulence—In *Self-Sustaining Mechanisms in Wall Turbulence*, R. L. Panton, ed. Southampton, UK: Computational Mechanics Publications, 109–134 (1997)	Feb. 1997

List of Recent TAM Reports (cont'd)

No.	Authors	Title	Date
846	Lufrano, J. M., P. Sofronis, and H. K. Birnbaum	Elastoplastically accommodated hydride formation and embrittlement—*Journal of Mechanics and Physics of Solids*, in press (1998)	Feb. 1997
847	Keane, R. D., N. Fujisawa, and R. J. Adrian	Unsteady non-penetrative thermal convection from non-uniform surfaces—In *Geophysical and Astrophysical Convection*, R. Kerr, ed. (1997)	Feb. 1997
848	Aref, H., and M. Brøns	On stagnation points and streamline topology in vortex flows—*Journal of Fluid Mechanics* **370**, 1–27 (1988)	Mar. 1997
849	Asghar, S., T. Hayat, and J. G. Harris	Diffraction by a slit in an infinite porous barrier—*Wave Motion*, in press (1998)	Mar. 1997
850	Shawki, T. G., H. Aref, and J. W. Phillips	Mechanics on the Web—Proceedings of the International Conference on Engineering Education (Aug. 1997, Chicago)	Apr. 1997
851	Stewart, D. S., and J. Yao	The normal detonation shock velocity–curvature relationship for materials with non-ideal equation of state and multiple turning points—*Combustion and Flame*, in press (1998)	Apr. 1997
852	Fried, E., A. Q. Shen, and S. T. Thoroddsen	Wave patterns in a thin layer of sand within a rotating horizontal cylinder—*Physics of Fluids* **10**, 10–12 (1998)	Apr. 1997
853	Boyland, P. L., H. Aref, and M. A. Stremler	Topological fluid mechanics of stirring	Apr. 1997
854	Parker, S. J., and S. Balachandar	Viscous and inviscid instabilities of flow along a streamwise corner—*Theoretical and Computational Fluid Dynamics*, in press (1997)	May 1997
855	Soloff, S. M., R. J. Adrian, and Z.-C. Liu	Distortion compensation for generalized stereoscopic particle image velocimetry—*Measurement Science and Technology* **8**, 1–14 (1997)	May 1997
856	Zhou, Z., R. J. Adrian, S. Balachandar, and T. M. Kendall	Mechanisms for generating coherent packets of hairpin vortices in near-wall turbulence—*Journal of Fluid Mechanics*, in press (1997)	June 1997
857	Neishtadt, A. I., D. L. Vainshtein, and A. A. Vasiliev	Chaotic advection in a cubic stokes flow—*Physica D* **111**, 227 (1997).	June 1997
858	Weaver, R. L.	Ultrasonics in an aluminum foam—*Ultrasonics*, in press (1997)	July 1997
859	Riahi, D. N.	High gravity convection in a mushy layer during alloy solidification—In *Nonlinear Instability, Chaos and Turbulence*, D. N. Riahi and L. Debnath, eds., in press (1998)	July 1997
860	Najjar, F. M., and S. Balachandar	Low-frequency unsteadiness in the wake of a normal plate, *Journal of Fluid Mechanics*, in press (1997)	Aug. 1997
861	Short, M.	A parabolic linear evolution equation for cellular detonation instability	Aug. 1997
862	Short, M., and D. S. Stewart	Cellular detonation stability—I: A normal-mode linear analysis	Sept. 1997
863	Carranza, F. L., and R. B. Haber	A numerical study of intergranular fracture and oxygen embrittlement in an elastic–viscoplastic solid—*Journal of the Mechanics and Physics of Solids*, in press (1997)	Oct. 1997
864	Sakakibara, J., and R. J. Adrian	Whole-field measurement of temperature in water using two-color laser-induced fluorescence	Oct. 1997
865	Riahi, D. N.	Effect of surface corrugation on convection in a three-dimensional finite box of fluid-saturated porous material	Oct. 1997
866	Baker, C. F., and D. N. Riahi	Three-dimensional flow instabilities during alloy solidification	Oct. 1997
867	Fried, E.	Introduction (only) to *The Physical and Mathematical Foundations of the Continuum Theory of Evolving Phase Interfaces* (book containing 14 seminal papers dedicated to Morton E. Gurtin), Berlin: Springer-Verlag, in press (1998)	Oct. 1997
868	Folguera, A., and J. G. Harris	Coupled Rayleigh surface waves in a slowly varying elastic waveguide	Oct. 1997

List of Recent TAM Reports (cont'd)

No.	*Authors*	*Title*	*Date*
869	Stewart, D. S.	Detonation shock dynamics: Application for precision cutting of metal with detonation waves	Oct. 1997
870	Shrotriya, P., and N. R. Sottos	Creep and relaxation behavior of woven glass/epoxy substrates for multilayer circuit board applications	Nov. 1997
871	Riahi, D. N.	Boundary wave–vortex interaction in channel flow at high Reynolds numbers, *Fluid Dynamics Research,* in press (1998)	Nov. 1997
872	George, W. K., L. Castillo, and M. Wosnik	A theory for turbulent pipe and channel flows—paper presented at *Disquisitiones Mechanicae* (Urbana, Ill., October 1996)	Nov. 1997
873	Aslam, T. D., and D. S. Stewart	Detonation shock dynamics and comparisons with direct numerical simulation	Dec. 1997
874	Short, M., and A. K. Kapila	Blow-up in semilinear parabolic equations with weak diffusion	Dec. 1997
875	Riahi, D. N.	Analysis and modeling for a turbulent convective plume—*Applied Mathematics Letters,* in press (1998)	Jan. 1998
876	Stremler, M. A., and H. Aref	Motion of three point vortices in a periodic parallelogram	Feb. 1998
877	Dey, N., K. J. Hsia, and D. F. Socie	On the stress dependence of high-temperature static fatigue life of ceramics	Feb. 1998
878	Brown, E. N., and N. R. Sottos	Thermoelastic properties of plain weave composites for multilayer circuit board applications	Feb. 1998
879	Riahi, D. N.	On the effect of a corrugated boundary on convective motion	Feb. 1998
880	Riahi, D. N.	On a turbulent boundary layer flow over a moving wavy wall	Mar. 1998
881	Riahi, D. N.	Vortex formation and stability analysis for shear flows over combined spatially and temporally structured walls	June 1998
882	Short, M., and D. S. Stewart	The multi-dimensional stability of weak heat release detonations	June 1998
883	Fried, E., and M. E. Gurtin	Coherent solid-state phase transitions with atomic diffusion: A thermomechanical treatment—*Journal of Statistical Physics* (1998)	June 1998
884	Langford, J. A., and R. D. Moser	Optimal large-eddy simulation formulations for isotropic turbulence	July 1998
885	Riahi, D. N.	Boundary-layer theory of magnetohydrodynamic turbulent convection	Aug. 1998
886	Riahi, D. N.	Nonlinear thermal instability in spherical shells	Aug. 1998
887	Riahi, D. N.	Effects of rotation on fully non-axisymmetric chimney convection during alloy solidification	Sept. 1998
888	Fried, E., and S. Sellers	The Debye theory of rotary diffusion	Sept. 1998
889	Short, M., A. K. Kapila, and J. J. Quirk	The hydrodynamic mechanisms of pulsating detonation wave instability	Sept. 1998
890	Stewart, D. S.	The shock dynamics of multidimensional condensed and gas phase detonations	Sept. 1998
891	Kim, K. C., and R. J. Adrian	Very large-scale motion in the outer layer	Oct. 1998
892	Fujisawa, N., and R. J. Adrian	Three-dimensional temperature measurement in turbulent thermal convection by extended range scanning liquid crystal thermometry	Oct. 1998
893	Shen, A. Q., E. Fried, and S. T. Thoroddsen	Is segregation-by-particle-type a generic mechanism underlying finger formation at fronts of flowing granular media?	Oct. 1998
894	Shen, A. Q.	Mathematical and analog modeling of lava dome growth	Oct. 1998
895	Buckmaster, J. D., and M. Short	Cellular instabilities, sub-limit structures, and edge-flames in premixed counterflows	Oct. 1998